of magnetic moments, transition moments, and spin densities using these wave functions.

Acknowledgment. This research was supported by the National Science Foundation under Grant CHE-8312286 and by Cray Research Inc. under a Cray Software Development Grant. We thank Dr. W. H. Miller and the Department of Chemistry, University of California, Berkeley, for their hospitality during the time that most of this work was carried out. Initial calculations were performed on the Cray X-MP/48 at the Pittsburgh Supercomputing Center and the Cray X-MP/24 at the Ohio Supercomputer Center. Most of the calculations were performed on the Cray X-MP/14 at the University of California, Berkeley, with a final set done on the Cray X-MP/416 at Cray Research Inc. We thank Dr. P. A. Christiansen for providing us with the uranium core potential and spin-orbit operators, and we thank Drs. N. Edelstein, A. Streitwieser, K. S. Pitzer, and K. N. Raymond for their help and advice.

Registry No. $U(C_8H_8)_2$, 11079-26-8.

Energetics and Hydration of the Constituent Ion Pairs of Tetramethylammonium Chloride

J. Kathleen Buckner and William L. Jorgensen*

Contribution from the Department of Chemistry, Purdue University, West Lafayette, Indiana 47907. *Received August 24, 1988*

Abstract: Statistical perturbation theory and Monte Carlo simulations have been utilized to obtain interionic potentials of mean force for the constituent ion pairs of tetramethylammonium chloride in dilute aqueous solution at 25 °C and 1 atm. For $(CH_3)_4N^+Cl^-$, a contact ion pair is found at an N–Cl distance of 5.0 Å and a broad minimum for the solvent separated form is centered near 7.5 Å. The two species are separated by a barrier of only 0.7 kcal/mol. From the calculated potential of mean force, the association constant for dilute aqueous $(CH_3)_4N^+Cl^-$ was determined to be 0.30 L/mol. For two chloride ions in water, a deep minimum is found at an interionic separation of 4.8–5.0 Å with a barrier to dissociation of ca. 6 kcal/mol. Though this result is qualitatively consistent with earlier findings, the possibility of a computational artifact is considered. The stability of the "solvent-bridged" ion pair can be attributed to the presence of three water molecules that simultaneously hydrogen bond to both chloride ions. In contrast, the approach of the other like ion pair, $(CH_3)_4N^+\cdots(CH_3)_4N^+$, is predicted to be purely repulsive. The energetic results are accompanied by details on the variation in solvation as a function of interionic separation.

The study of aqueous electrolyte solutions on a molecular level has revealed many properties of these systems not previously detected by theories that treat the solvent as a dielectric continuum. By examining the free energy as a function of the interionic distance or "potential of mean force" (pmf), statistical mechanical theories have been able to better describe the detailed mechanisms of ion pairing in solution. For example, integral equation studies of alkali halides in water have found oscillatory behavior in the pmfs for the anion–cation interactions.[1-3] A molecular dynamics calculation on aqueous NaCl[4] and a Monte Carlo study of aqueous *tert*-butyl chloride[5] showed the same behavior and clearly identified minima corresponding to contact and solvent-separated ion pairs. In the integral equation studies, cation–cation pmfs were also found to have modest minima that were not stabilized with respect to infinite separation.[1-3] Recently, an extended RISM treatment of dilute aqueous alkali halides[6] and a molecular dynamics simulation of two chloride ions in water[7,8] that used the same potential function model gave evidence for the existence of chloride ion pairs stabilized near contact in aqueous solution. The stability of these anionic pairs was attributed to bridging structures in which water molecules can hydrogen bond to both chloride ions simultaneously. Subsequently, the reference hypernetted chain (RHNC) approximation has been applied to aqueous ionic solutions at infinite dilution and finite concentrations.[9] The model consisted of hard sphere ions in a solvent of hard multipolar polarizable particles and corresponded to some alkali halides and $(C_2H_5)_4NBr$ in water. This study found contact and solvent-separated minima in the pmfs for the unlike-charged ions, though the solvent-separated minimum for Et_4NBr was very shallow. Attractive wells were also detected for the smaller like-charged ion pairs, both negative and positive. Due to the nature of the solvent model, the pmfs for the same size cations and anions are identical.

The association constant, K_a, is another property of salt solutions that can be better described with molecular models for the solvent. Bjerrum theory,[10] which has long been used to obtain association constants for infinitely dilute solutions, fails in many areas because it depends only on properties of the ions and on the dielectric constant of the solvent. For example, the theory predicts the association constants for tetraalkylammonium salts to decrease with increasing size in protic solvents. This trend is observed in alcoholic solvents, but the reverse trend occurs in water.[11] The reversal has been attributed to water structure-enforced ion pairing[12] in which larger, more hydrophobic ions are forced into the same cage by the solvent in order to decrease the disruption of the hydrogen-bonded network of water. A theoretical treatment of K_a that utilizes a molecular interpretation of the solvent should be able to explain such effects. In fact, an extended RISM study[13] of ion pairs in alcoholic solvents yielded trends in K_a's at infinite

(1) Patey, G. N.; Carnie, S. L. *J. Chem. Phys.* **1983**, *78*, 5183.
(2) Kusalik, P. G.; Patey, G. N. *J. Chem. Phys.* **1983**, *79*, 4468.
(3) Hirata, F.; Rossky, P. J.; Pettitt, B. M. *J. Chem. Phys.* **1983**, *78*, 4133.
(4) Berkowitz, M.; Karim, O. A.; McCammon, J. A.; Rossky, P. J. *Chem. Phys. Lett.* **1984**, *105*, 577. Belch, A. C.; Berkowitz, M.; McCammon, J. A. *J. Am. Chem. Soc.* **1986**, *108*, 1755. Karim, O. A.; McCammon, J. A. *J. Am. Chem. Soc.* **1986**, *108*, 1762.
(5) Jorgensen, W. L.; Buckner, J. K.; Huston, S. E.; Rossky, P. J. *J. Am. Chem. Soc.* **1987**, *109*, 1891.
(6) Pettitt, B. M.; Rossky, P. J. *J. Chem. Phys.* **1986**, *84*, 5836.
(7) Dang, L. X.; Pettitt, B. M. *J. Am. Chem. Soc.* **1987**, *109*, 5531.
(8) Dang, L. X.; Pettitt, B. M. *J. Chem. Phys.* **1987**, *86*, 6560.
(9) Kusalik, P. G.; Patey, G. N. *J. Chem. Phys.* **1988**, *88*, 7715.
(10) Davies, C. W. *Ion Association*; Butterworths Scientific Publications: London, 1962.
(11) Accascina, F.; Goffredi, M.; Triolo, R. *Z. Phys. Chem. Neu. Fol.* **1972**, *81*, 148.
(12) Diamond, R. M. *J. Phys. Chem.* **1963**, *67*, 2513.
(13) Hirata, F.; Levy, R. M. *J. Phys. Chem.* **1987**, *91*, 4788.

0002-7863/89/1511-2507$01.50/0

dilution in agreement with experiment that could not be predicted by Bjerrum theory,

In view of these considerations, the general lack of knowledge about interionic potentials of mean force, and the wide-ranging importance of aqueous electrolyte solutions,[14] extension of the theoretical studies to better understand their characteristics and to examine a greater variety of ion pairs is called for. The preferred procedures are molecular dynamics (MD) or Monte Carlo (MC) statistical mechanics simulations for the ion pairs with explicit inclusion of hundreds of solvent molecules. Though the integral equation calculations require far less computer time, the results are an approximation to the solution of the full statistical mechanical problem, and it appears that they often yield pmfs with diminished structure relative to the MD or MC findings.[4-6] Consequently, we have performed Monte Carlo simulations to study the hydration and aqueous pmfs for the three constituent ion pairs of tetramethylammonium chloride, as reported here. This prototypical tetraalkylammonium salt provides a particularly attractive model system since a variety of forces is embodied including hydrogen bonding, and electrostatic and hydrophobic interactions. Parallels have also been found between the effects of solvation on tetramethylammonium chloride and the transition state for solvolysis of *tert*-butyl chloride,[15] which provides a connection to our previous study.[5] Moreover, alkylammonium ions are components of some biologically important molecules such as phospholipids, so a knowledge of the behavior of the simple prototype provides a useful reference point.

Tetraalkylammonium salts have been studied by many experimental methods. Solvent structural effects have been found to play an important role in these systems.[16] Experiments on thermodynamic and transport properties as well as spectroscopic studies of aqueous tetraalkylammonium salts have uncovered some interesting properties of the ion pairing. For example, studies of volume[17] and free energy changes[18] upon mixing tetraalkylammonium halide and alkali halide solutions have suggested the occurrence of pairing between the tetraalkylammonium ions. The effect was found to be most pronounced for the larger cations, perhaps ten times as great for Bu_4N^+ as for $(CH_3)_4N^+$. Studies of the temperature and concentration dependence of isothermal transport properties of alkylammonium salts indicated the presence of cationic pairs, though for $(CH_3)_4N^+$ the ion pairs were only found at concentrations greater than 2 M.[19] Measurements of the salting in of nonelectrolytes by various salt solutions suggest that the behavior of $(CH_3)_4N^+$ in aqueous solution is intermediate between that of alkali ions and the larger tetraalkylammonium ions,[20] Finally, an investigation of the proton and deuteron nuclear magnetic relaxation rate of some tetraalkylammonium chlorides found evidence for cationic pairing in aqueous solutions of Et_4NCl, but not in aqueous solutions of Me_4NCl.[21] The association of alkylammonium ions in aqueous solution has been attributed to the hydrophobic effect. For the larger species, hydrophobicity is claimed to overshadow the electrostatic repulsion. However, for $(CH_3)_4N^+$ the two forces are apparently more in balance. It is also worth reexamining the interanionic interactions in solution in light of the striking results for $Cl^-\cdots Cl^-$ mentioned above from integral equation theories and molecular dynamics. Experimental support has been given for the possibility of anionic association in solution.[22] Interpretation of velocity correlation coefficients for aqueous tetraalkylammonium bromides indicated correlations between the motions of both cations and anions in the larger salts,[22a] and NMR relaxation data for aqueous alkali halides have implicated anion pairing.[22b] However, Zhong and Friedman find that chloride ion pairing in water, as embodied in the pmfs from the integral equation calculations,[6] is inconsistent with their analyses of the distinct diffusion coefficient.[23]

The present study addresses these fundamental questions about interionic interactions as well as the details of hydration for the ion pairs. The interionic potentials of mean force were obtained from statistical perturbation theory in conjunction with Monte Carlo simulations and permitted calculation of the association constant for tetramethylammonium chloride. The only comparable prior studies were the MD and MC calculations for the pmfs of NaCl, Cl_2^{2-}, and $(CH_3)_3CCl$.[4,5,7]

Computational Procedure

The procedure used here is similar to that employed to study the energetics and hydration of aqueous *tert*-butyl chloride ion pairs.[5] The modeled system consisted of the solutes plus either 250 or 750 water molecules in a rectangular box with periodic boundary conditions. First, a brief discussion of the potential functions is given and then the statistical mechanical calculations are described, including a summary of the method for computing the association constant.

Potential Functions. The nonbonded interactions are described in a Coulomb plus Lennard-Jones format (eq 1) where the sums are over sites located on the ions and water molecules. The four-site TIP4P model was

$$\Delta E_{ab} = \sum_{i}^{\text{on a}} \sum_{j}^{\text{on b}} (q_i q_j e^2/r_{ij} + A_{ij}/r_{ij}^{12} - C_{ij}/r_{ij}^{6}) \qquad (1)$$

used for the water,[24] while the ions were described by the OPLS parameters, also reported previously.[25] The tetramethylammonium ion is represented by five sites centered on the nitrogen and carbon atoms with $q(CH_3) = +0.25$ and $r(C-N) = 1.51$ Å. The Lennard-Jones σ and ϵ for CH_3 are 3.96 Å and 0.145 kcal/mol, and for N, 3.25 Å and 0.170 kcal/mol. The single site for chloride ion has a charge of −1, $\sigma = 4.471$ Å, and $\epsilon = 0.118$ kcal/mol. These parameters have been shown to give excellent results for the thermodynamics of hydration for the single ions.[25]

Several more details should be noted. The A's and C's in eq 1 are related to the Lennard-Jones parameters by $A_{ii} = 4\epsilon_i\sigma_i^{12}$ and $C_{ii} = 4\epsilon_i\sigma_i^{6}$, and the combining rules are $A_{ij} = (A_{ii}A_{jj})^{1/2}$ and $C_{ij} = (C_{ii}C_{jj})^{1/2}$. These parameters and the charges are kept fixed so polarization effects are not explicitly included in the calculations, though they are reflected in the original parametrization in an average sense. The lack of instantaneous polarization is the largest concern for the accuracy of the results, though it is less problematic for the larger ions considered here than for smaller, more charge-localized ions.[5,25] Intramolecular vibrational effects are also not included since the bond lengths and angles for the individual water molecules and $(CH_3)_4N^+$ are held fixed. Finally, concern could be expressed for the ability of the parameters for the ions, which were developed to give a good description of ion–water interactions, to represent well the ion–ion interactions. This was tested for $Cl^-\cdots Cl^-$ by a series of high-level ab initio molecular orbital calculations. The energy was computed as a function of the interionic distance with the 6-31+G(d) basis set, which includes d orbitals and diffuse s and p orbitals, and with the correlation energy determined with Møller–Plesset theory at the MP4 level.[26] The results are described below.

Monte Carlo Simulations. The Monte Carlo simulations were performed for each of the ion pairs plus 250 water molecules in a rectangular box (ca. 17 × 17 × 26 Å) with periodic boundary conditions in the NPT ensemble at 25 °C and 1 atm. Statistical perturbation theory was used to obtain the potentials of mean force. This approach is based on eq 2

(14) Wolynes, P. G. *Annu. Rev. Phys. Chem.* **1980**, *31*, 325. Friedman, H. *Ibid.* **1981**, *32*, 179.
(15) Abraham, M. H. *J. Chem. Soc. Perkin Trans. II* **1972**, 1343.
(16) Wen, W. Y. *J. Solution Chem.* **1973**, *2*, 253.
(17) Wen, W. Y.; Nara, K.; Wood, R. H. *J. Phys. Chem.* **1968**, *72*, 3048. Wen, W. Y.; Nara, K. *J. Phys. Chem.* **1967**, *71*, 3907.
(18) Wen, W. Y.; Miyajima, K.; Otsuka, A. *J. Phys. Chem.* **1971**, *14*, 2148.
(19) Surdo, A. L.; Wirth, H. E. *J. Phys. Chem.* **1979**, *83*, 879.
(20) Wen, W. Y.; Hung, J. H. *J. Phys. Chem.* **1970**, *74*, 170.
(21) Hertz, H. G.; Lindman, B.; Siepe, V. *Ber. Bunsen-Ges. Phys. Chem.* **1969**, *73*, 542.
(22) (a) Woolf, L. A.; Weingartner, H. *Faraday Sym. Chem. Soc.* **1982**, *17*, 41. (b) Hertz, H. G.; Rödel, C. *Ber. Bunsen-Ges. Phys. Chem.* **1974**, *78*, 509.
(23) Zhong, E. C.; Friedman, H. L. *J. Phys. Chem.* **1988**, *92*, 1685.
(24) (a) Jorgensen, W. L.; Chandrasekhar, J.; Madura, J. D.; Impey, R. W.; Klein, M. L. *J. Chem. Phys.* **1983**, *79*, 926. (b) Jorgensen, W. L.; Madura, J. D. *Mol. Phys.* **1983**, *56*, 1381. (c) Neumann, M. J. *J. Chem. Phys.* **1986**, *85*, 1567.
(25) (a) Jorgensen, W. L.; Gao, J. *J. Phys. Chem.* **1986**, *90*, 2174. (b) Chandrasekhar, J.; Spellmeyer, D. C.; Jorgensen, W. l. *J. Am. Chem. Soc.* **1984**, *106*, 903. (c) Jorgensen, W. L.; Buckner, J. K.; Blake, J. M. *Chem. Phys.* **1989**, *129*, 193.
(26) Hehre, W. J.; Radom, C.; Schleyer, P. v. R.; Pople, J. A. *Ab. Initio Molecular Orbital Theory*; Wiley: New York, NY, 1986. The calculations used the Gaussian 86 program: Frisch, M. J.; Binkley, J. S.; Schlegel, H. B.; Raghavachari, K.; Melius, C. F.; Martin, R. L.; Stewart, J. J. P.; Bobrowicz, F. W.; Rohlfing, C. M.; Kahn, L. R.; Defrees, K. J.; Seeger, R.; Whiteside, R. A.; Fox, D. J.; Fleuder, E. M.; Pople, J. A., Carnegie-Mellon Quantum Chemistry Publishing Unit, Pittsburgh, PA, 1986.

$$G_1 - G_0 = -k_B T \ln \langle \exp(-[H_1 - H_0]/k_B T) \rangle_0 \quad (2)$$

in which the free energy difference between a reference system, 0, and a perturbed system, 1, is given as a function of the average energy difference between the two systems.[27] The notation $\langle \cdots \rangle_0$ implies that the configurational sampling is based on the reference system. A series of simulations is then performed at points along the reaction path, and the resulting free energy changes are accumulated to yield the potential of mean force. Care must be taken not to make the perturbations too large in order to obtain convergence of eq 2. Double-wide sampling in which the reference system is perturbed in both directions along the reaction path was used in order to minimize the number of simulations required.[28]

Three series of simulations were performed; one in which the N–Cl distance in the $(CH_3)_4N^+Cl^-$ ion pair was perturbed from 4.25 to 8.75 Å in increments of 0.25 Å, a second in which the $Cl^-\cdots Cl^-$ distance was changed from 3.4 to 8.2 Å in increments of 0.2 Å, and a third in which the N–N distance in $(CH_3)_4N^+\cdots(CH_3)_4N^+$ was perturbed from 4.8 to 7.2 Å in steps of 0.2 Å. Each simulation involved equilibration for 6×10^5 to 8×10^5 configurations followed by averaging for 1.5×10^6 or 1.6×10^6 configurations. In order to test the size and cutoff dependence of the results, two additional calculations were performed for the chloride ion pair in a box containing 750 water molecules (ca. $25 \times 25 \times 37$ Å) near the minimum determined from the smaller system. For these simulations, equilibration was carried out for 1.5×10^6 configurations followed by averaging for 2.5×10^6 configurations. Preferential sampling was used with the Metropolis algorithm to enhance convergence.[29,30] Cutoffs for interactions between molecules were handled as in our previous study of aqueous ion pairs[5] with a procedure similar to Andersen's.[31] Specifically, the interaction energy between a molecule or ion and the surrounding particles is scaled to zero quadratically over 0.5 Å approaching the cutoff. Cutoffs for solute–solvent interactions were based on each solute site–water O distance and water–water cutoffs were based on the O–O distance. The cutoffs were 8.5 Å for the smaller system and 10.5 Å for the larger system. In the simulations, the solvent molecules could translate and rotate randomly. The ion pairs were allowed to translate randomly in tandem and the $(CH_3)_4N^+$ ions were allowed to independently rotate. Ranges for the movements were chosen such that an acceptance rate of 40% for new configurations was attained. The solute and volume moves were attempted every 60 and 1500 configurations, respectively. The calculations were carried out with the BOSS program, version 2.0, on Sun 4 computers.

The association constant for a pair of ions in an ideal solution is defined by eq 3, where α is the degree of association and c_0 is the initial

$$K_a = \alpha/[(1 - \alpha)^2 c_0] \quad (3)$$

concentration of the salt.[32] The degree of association is given by eq 4 where $w(r)$ is the solvent mediated potential of mean force and r_c is the

$$\alpha = c_0 \int_0^{r_c} 4\pi r^2 \exp(-[w(r)/k_B T]) \, dr \quad (4)$$

geometric limit for association. For very dilute solutions, α is small and equilibrium constant reduces to eq 5. Thus, the potential of mean force

$$K_a = \alpha/c_0 = \int_0^{r_c} 4\pi r^2 \exp(-[w(r)/k_B T]) \, dr \quad (5)$$

from the Monte Carlo calculations can readily be used to calculate the association constant at infinite dilution. This method was employed to calculate K_a for NaCl in alcoholic solvents from the results of extended RISM calculations.[13] The effect of the cutoff limit on the calculated association constant was examined and the results were compared to those from the Bjerrum theory.

Results and Discussion

Tetramethylammonium Chloride. A. Potential of Mean Force and K_a. The computed potential of mean force for $(CH_3)_4NCl$ is plotted in Figure 1 along with the "primitive model" result. The latter is obtained from the bare ion–ion interaction by dividing the Coulombic contribution by the experimental dielectric constant of water.[5,6] The simulation results were anchored to the primitive model at r(N–Cl) = 8.75 Å. Table I gives the free energy change calculated at each step and the resulting cumulative free energy changes. Standard deviations ($\pm 1\sigma$) obtained from averages over blocks of 1×10^5 configurations are also listed in the table. The cumulative uncertainty at the endpoints of the pmf relative to the middle is estimated from the fluctuations to be ca. ±0.4 kcal/mol.

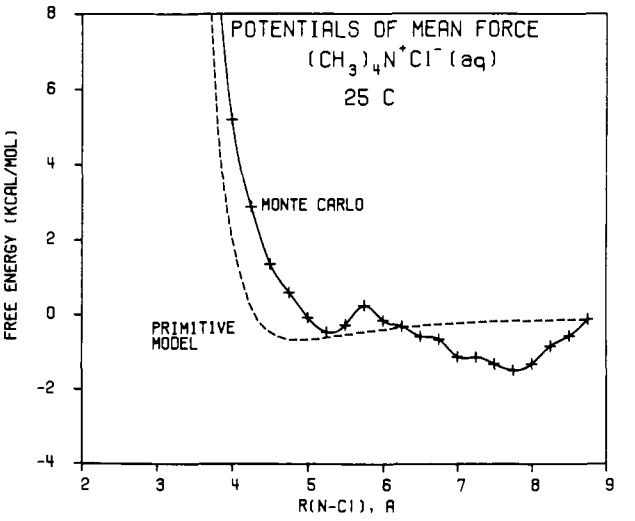

Figure 1. Calculated potentials of mean force for $(CH_3)_4N^+\cdots Cl^-$ in water.

Table I. Results for the $(CH_3)_4N^+\cdots Cl^-$ Potential of Mean Force from the Monte Carlo Simulations[a]

r(N–Cl)		ΔG		
r_i	r_j	$i \rightarrow j$	$j \rightarrow i$	$\Delta G^{tot}(r_i)$
3.75	4.00		4.95 ± 0.18	10.29
4.00	4.25	−2.33 ± 0.19		5.34
4.25	4.50		1.53 ± 0.16	3.01
4.50	4.75	−0.77 ± 0.19		1.48
4.75	5.00		0.66 ± 0.17	0.71
5.00	5.25	−0.39 ± 0.16		0.05
5.25	5.50		−0.19 ± 0.10	−0.34
5.50	5.75	0.52 ± 0.15		−0.15
5.75	6.00		0.40 ± 0.18	0.37
6.00	6.25	−0.16 ± 0.20		−0.03
6.25	6.50		0.27 ± 0.15	−0.19
6.50	6.75	−0.08 ± 0.23		−0.46
6.75	7.00		0.47 ± 0.15	−0.54
7.00	7.25	−0.01 ± 0.12		−1.01
7.25	7.50		0.18 ± 0.15	−1.02
7.50	7.75	−0.17 ± 0.14		−1.20
7.75	8.00		−0.17 ± 0.14	−1.37
8.00	8.25	0.48 ± 0.15		−1.20
8.25	8.50		−0.27 ± 0.10	−0.72
8.50	8.75	0.45 ± 0.13		−0.45

[a] Distances in Å; energies in kcal/mol.

Two minima are apparent in the pmf corresponding to contact and solvent-separated ion pairs. The two species are isolated by a barrier of only 0.7 kcal/mol. The contact minimum is located at an N–Cl separation of ca. 5.25 Å, a substantially larger separation than predicted by the primitive model. This effect is consistent with steric screening of the chloride ion by the tetramethylammonium ion at shorter distances. By keeping the ions farther apart, the chloride ion can retain close to the 7–8 hydrogen bonds that are computed for it when isolated in water.[5,25b,33] The last configuration from the Monte Carlo simulation at 5.0 Å is shown in Figure 2. It can be seen that near the contact minimum,

(27) For a review, see: Mezei, M.; Beveridge, D. L. *Ann. N.Y. Acad. Sci.* **1986**, *482*, 1.
(28) Jorgensen, W. L.; Ravimohan, C. *J. Chem. Phys.* **1985**, *83*, 3050.
(29) Owicki, J. C. *Am. Chem. Soc. Symp. Ser.* **1978**, *86*, 159.
(30) Metropolis, N.; Rosenbluth, A. W.; Rosenbluth, M. N.; Teller, A. H.; Teller, E. *J. Chem. Phys.* **1953**, *21*, 1087.
(31) Andrea, T. A.; Swope, W. C.; Ansersen, H. C. *J. Chem. Phys.* **1983**, *79*, 4576.
(32) Conway, B. E. *Ionic Hydration in Chemistry and Biophysics*; Elsevier Scientific Publishing Co.: Amsterdam, 1981.

(33) It should be noted that the highest hydration number observed so far in diffraction data for Cl^- is 5.9 ± 0.2 (Enderby, J. E.; Cummings, S.; Herdman, G. J.; Neilson, G. W.; Salmon, P. S.; Skipper, N. *J. Phys. Chem.* **1987**, *91*, 5851). This is still in relatively concentrated aqueous solution (3.6 m) with a highly electrophilic counterion (Li^+).

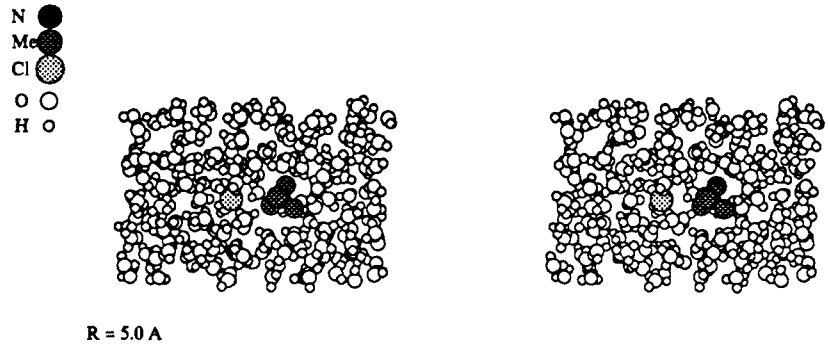

Figure 2. Stereoplot of a configuration for the $(CH_3)_4N^+Cl^-$ contact ion pair at an N–Cl separation of 5.0 Å. Water molecules more than 4.5 Å in front of the chlorine have been deleted for clarity of viewing.

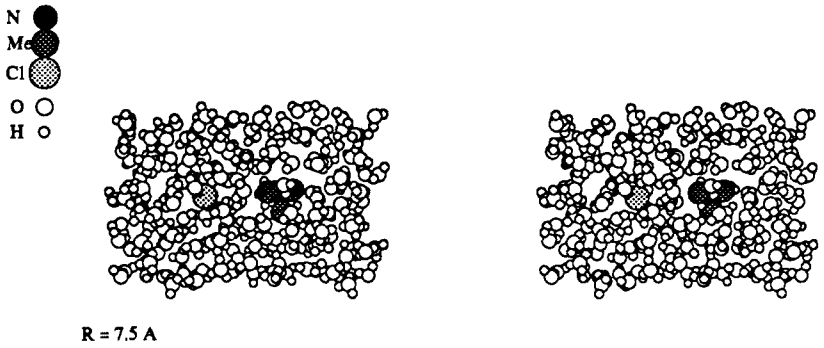

Figure 3. Stereoplot of the $(CH_3)_4N^+Cl^-$ solvent-separated ion pair at an N–Cl separation of 7.5 Å. Details as in Figure 2.

6–7 water molecules are still able to hydrogen bond to the chloride ion without any of them actually moving between the two ions. The plot of a configuration at an interionic distance of 7.5 Å in Figure 3 shows a layer of favorably oriented water molecules between the ions for the solvent-separated ion pair. At this point the chloride ion has its full complement of hydrogen bonds. More details on the hydration are provided below.

The pmf in Figure 1 from the simulations is less structured than that for the *tert*-butyl chloride ion pair for which the well-depth for the contact ion pair was ca. 2 kcal/mol and the free energy difference between the two minima was ca. 4 kcal/mol favoring the solvent-separated form.[5] The ion–water interactions for the planar $(CH_3)_3C^+$ ion are more sensitive to orientation than for the more spherical $(CH_3)_4N^+$, The drive to have a water molecule on either side of the central carbon for *tert*-butyl cation is probably responsible for the difference in pmfs. These interactions are bonding by ca. 15 kcal/mol,[5] while the most favorable $(CH_3)_4N^+$–water interaction is only −10 kcal/mol with the present potential functions. The pmf for $(CH_3)_4N^+\cdots Cl^-$ is also relatively flat compared to the MD results for $Na^+\cdots Cl^-$.[4] In that case, the computed barrier between the two minima is ca. 3 kcal/mol and the contact ion pair is ca. 1.3 kcal/mol below the solvent-separated form. A major difference is that the positions of the minima are at ca. 2.5 Å smaller separation for $Na^+\cdots Cl^-$ than in Figure 1 owing to the difference in size of the cations. For aqueous Et_4NBr, the RHNC treatment found a contact minimum with a depth of ca. 2.2 kcal/mol and a very shallow solvent-separated minimum.[9] Though the model used in that study was much simpler than the one employed here, the relative depths of the contact minima from the two studies support the notion that association between the larger ions is favored by water structure-enforced ion pairing.

The pmf from the simulations was then used to compute the association constant for $(CH_3)_4NCl$ at infinite dilution via eq 5. The results are shown in Figure 4 as a function of r_c. The natural choice for r_c would be at the position of the barrier top between the contact and solvent-separated ion pairs, which is consistent with the spectroscopic definition of associated ions.[32] Integration to this point (5.75 Å) yields a K_a of 0.30 M^{-1}. The experimental association constant obtained from conductance data is 0.8 ± 0.2 M^{-1}.[11] This value is matched in Figure 4 by choosing r_c to be 7.2 Å. The results for K_a are clearly very sensitive to r_c. Nevertheless,

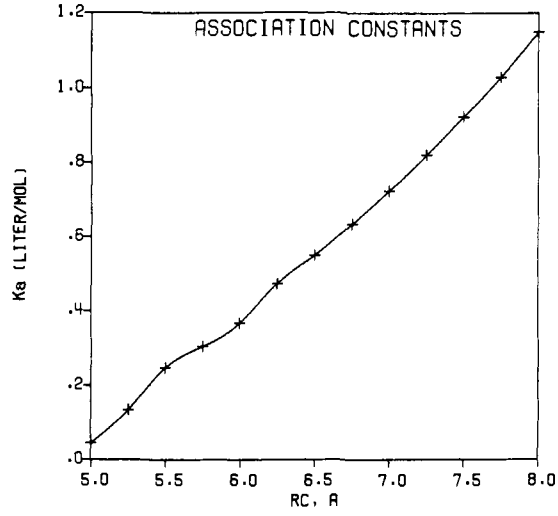

Figure 4. Association constant for $(CH_3)_4N^+Cl^-$ vs cutoff, r_c, computed from eq 5.

theory and experiment concur that tetramethylammonium chloride has a relatively small K_a comparable to that for $KClO_3$ (K_a = 0.8).[34] In contrast, the K_a's for less soluble salts such as AgOAc and AgCl are 5 and 1600.[34]

B. Bonding Energy Distributions. More details on the energetics of solvation are available from the distribution functions in Figures 5 and 6. Figure 5 displays the distributions of total ion pair–water interaction energies at four N–Cl distances, 5.0 Å (near the contact minimum), 6.0 Å (in the barrier region), 7.0 Å (in the solvent-separated well), and 8.5 Å (the largest separation studied). In each case, a substantial range of energetic environments is sampled covering at least 50 kcal/mol. As the ions separate, the total ion–water interaction energy decreases substantially from about −175 kcal/mol at 5 Å to −225 kcal/mol at 8.5 Å. Of course, the ion–ion attraction simultaneously becomes less favorable by ca.

(34) Bjerrum, J.; Schwarzenbach, G.; Sillen, L. G. *Stability Constants*; Chemical Society: London, 1958.

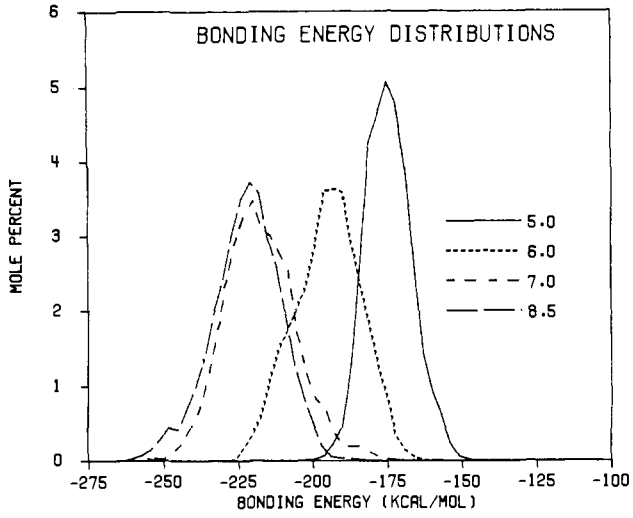

Figure 5. Total ion pair–solvent bonding energies for $(CH_3)_4N^+Cl^-$ in water. The different curves are for the indicated N–Cl distances. Units for the ordinate are mol % per kcal/mol.

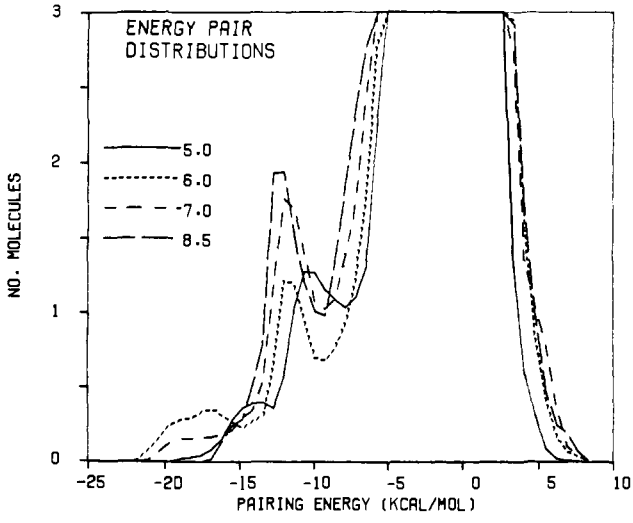

Figure 6. Distributions of individual water–ion pair interaction energies. Units for the ordinate are number of water molecules per kcal/mol.

27 kcal/mol over this range and there is greater solvent disruption (loss of water–water hydrogen bonds and decreased solvent entropy) as the ions become better hydrated. The balance of these effects is remarkable and yields the relatively flat pmf beyond 5 Å in Figure 1. The comparative constancy of the distributions in Figure 5 at 7 and 8.5 Å is consistent with ideas from theories on hydration cosphere overlap.[35] In the solvent-separated region and beyond, solvent molecules between the ions can orient relatively favorably with respect to both; however, at smaller separations these well-bound solvent molecules are forced into less favorable orientations.

This effect is also revealed in the energy pair distributions shown in Figure 6. The plots give the number of individual water–ion pair interactions with the interaction energy on the abscissa. The most attractive interactions are −19 to −22 kcal/mol, occur at intermediate separations (6–7 Å), and correspond to water molecules between the ions while the ions are still relatively close. Overall, there are three principal bands in the figure: the lowest energy can be assigned to the water molecules that interact very favorably with both ions, the band centered near −12 kcal/mol is attributable to water molecules interacting primarily with the chloride ion through hydrogen bonds, and the wide band centered near 0 kcal/mol is for the interactions with the many water molecules outside of the first solvent layer. The contributions from the water molecules that interact primarily with the tetramethylammonium ion are buried in the −5 to −10 kcal/mol region of the wide band. The two low-energy bands for r(N–Cl) = 5 Å are shifted to higher energy owing to the difficulties in achieving as favorable orientations when the ions are very close.

(35) Ramanathan, P. S.; Krishnan, C. V.; Friedman, H. L. *J. Solution Chem.* **1972**, *3*, 237.

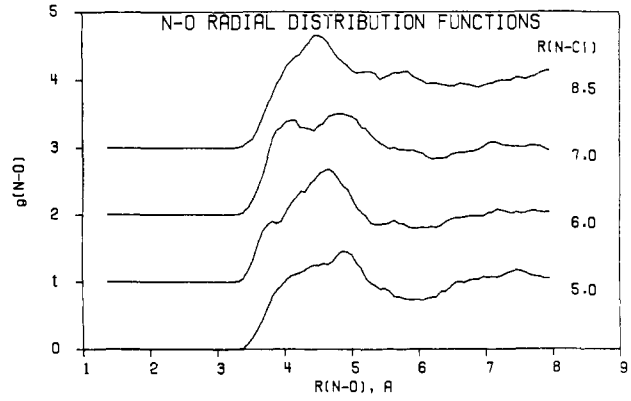

Figure 7. N (from Me_4NCl)–water O radial distribution functions computed in the simulations. Successive curves are offset 1 unit on the y axis.

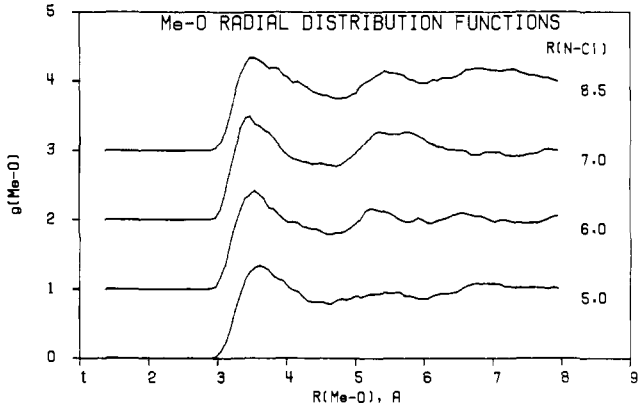

Figure 8. Computed methyl (from Me_4NCl)–water O radial distribution functions. Successive curves are offset 1 unit on the y axis.

Table II. Computed Hydration Numbers from Integrating the First Peak in the X–O Radial Distribution Functions[a]

r(N–Cl), Å	N–O	Me–O	Cl–O
4.0	3.5	7.4	6.4
4.5	4.2	8.3	6.8
5.0	4.5	7.5	6.4
5.5	5.2	8.7	6.6
6.0	5.2	8.6	7.3
6.5	4.7	8.1	7.4
7.0	5.8	8.7	7.8
7.5	5.7	8.2	7.9
8.0	5.2	9.0	8.0
8.5	5.1	8.6	7.0

[a] Cutoffs: N, 4.30 Å; Me, 4.50 Å; Cl, 3.85 Å.

C. **Atomic Distributions.** Solute–solvent radial distribution functions (rdfs) and results of proximity analyses were obtained in order to further characterize the solvation of the ion pairs. The computed N–O and CH_3–O rdfs are shown in Figures 7 and 8 for the same interionic separations as above. In all cases, the rdfs exhibit broad peaks and shallow minima reflecting a lack of orientational preference, though some interesting variations are apparent. The N–O rdfs all exhibit a broad band of hydration from 3.5 to 5.5 Å. The first component of the rdfs centered near 3.8 Å starts as a shoulder in the rdf for the contact pair and grows into a peak at the solvent-separated minimum (7.0 Å) and then becomes less distinct again at the largest separation. This can be attributed to water molecules that are squeezed between the two ions such that the water oxygens closely approach the cation

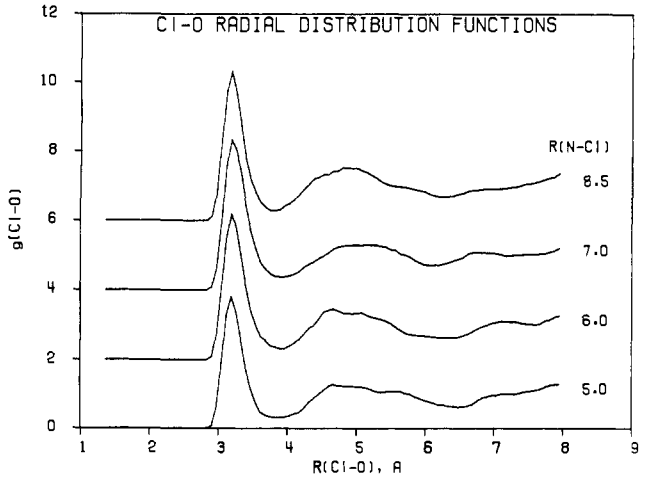

Figure 9. Computed Cl (from Me_4NCl)-water O radial distribution functions. Successive curves are offset 2 units on the y axis.

between the methyl groups. At smaller interionic distances water molecules cannot fit between the ions, while at greater separations the packing between the ions is not as constrained. Integration of the first band of the N–O rdf out to 4.3 Å indicates the number of water molecules in this feature grows from 3.5 at contact to a maximum of 5.8 in the solvent-separated well and then returns to 5.0 for the separated ions (Table II).

The CH_3–O (Figure 8) and CH_3–H radial distribution functions do not change significantly with the N–Cl separation and are quite similar to those for dilute aqueous tetramethylammonium ion.[24a] The first peaks in the CH_3–O rdfs are centered near 3.5 Å and those for the CH_3–H rdfs are centered near 4.0, consistent with the expected orientation for favorable electrostatic interactions. Integration of the first peak in the CH_3–O rdfs to the minimum located at ca. 4.5 Å indicates that the number of water neighbors for the methyl groups is between 7.5 and 9.0 over the range of interionic distances, with the smallest values occurring near contact. This trend is consistent with increased shielding of some of the methyl groups as the chloride ion approaches.

The locations of the peaks in the Cl–O (Figure 9) and Cl–H radial distribution functions are all similar to those determined for dilute aqueous chloride ion.[25b] The maximum in the first Cl–O peak is located at 3.2 Å and the maximum in the first Cl–H peak is centered around 2.3 Å, consistent with linear hydrogen bonding to water. Integration of the first peaks in the Cl–O rdfs out to the minimum at ca. 3.85 Å shows that the coordination number for the chloride ion grows from around 6.4 near contact to 7–8 in the solvent-separated region and beyond (Table II). Using the same potential functions, dilute aqueous chloride ion was previously found by Monte Carlo simulations to have a coordination number of 7–8.[25b]

The proximity analyses prescribed by Mehrotra and Beveridge can be used to further characterize the nature of the first solvation shells.[36] Each solute atom is assigned a maximum radius for its first hydration shell, which we take as the cutoff for the first peak in the solute atom–oxygen of water rdfs. Thus, if a water oxygen is within the cutoff for a solute atom and closer to that solute atom than any other solute atom, the water molecule is counted as in the solute atom's primary hydration shell. The solvent molecules to which a solute atom is second closest and still within the cutoff make up the secondary hydration molecules, and so on. The average interaction energies between the ion pair and the primary hydration molecules have also been calculated here. The analyses were performed on 20–50 configurations saved at regular intervals throughout the simulations. Uncertainties are estimated to be ca. ±0.5 for the coordination numbers and ca. ±1 kcal/mol for the average interaction energies.

The results are presented in Table III for the methyl groups and chloride ion in the ion pairs; the primary hydration shell for

(36) Mehrotra, P. K.; Beveridge, D. L. *J. Am. Chem. Soc.* **1980**, *102*, 4287.

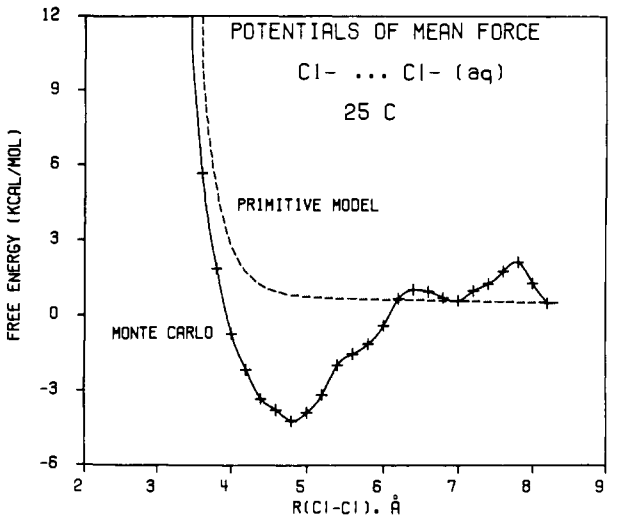

Figure 10. Calculated potentials of mean force for $Cl^-\cdots Cl^-$ in water.

Table III. Computed Primary Hydration Numbers and Ion Pair–Water Interaction Energies (kcal/mol) from Proximity Analyses[a]

	primary hydration no.		ion pair–water energy	
r(N–Cl), Å	Me	Cl	Me	Cl
4.0	4.4	6.0	−2.4	−9.6
4.5	4.6	6.3	−2.1	−10.3
5.0	3.6	6.1	−3.7	−10.4
5.5	4.4	6.3	−3.0	−11.3
6.0	4.5	6.8	−2.9	−11.4
6.5	4.4	6.8	−3.8	−11.7
7.0	5.0	7.4	−3.8	−11.2
7.5	4.5	7.7	−3.7	−11.1
8.0	5.1	7.8	−3.3	−11.2
8.5	5.3	6.6	−3.1	−11.8

[a] Cutoffs: Me, 4.50 Å; Cl, 3.85 Å.

N is empty because it is covered by the methyl groups. The methyl group primary coordination number fluctuates between 4 and 5, with the lowest values near contact. The average interaction energies for these water molecules with the ion pair are between −2.0 and −3.8 kcal/mol with the most favorable interactions occurring near the contact and solvent-separated minima. The favorable interactions for the solvent-separated ion pair confirm the assertion that the water molecules between the ions are particularly well bound. The chloride ion hydration number is again found to increase from a little more than 6 water molecules at contact to 7–8 for larger separations. The average interaction energy for these water molecules and the ion pair decreases from −9.6 to −11.8 kcal/mol as the ions separate. This trend can be attributed to a lessening of unfavorable interactions with the cation as the ions separate for most of the water molecules that are hydrogen bonding to the chloride ion.

The structural changes that occur as a function of ion separation are not as distinct for $(CH_3)_4N^+Cl^-$ as they are for $(CH_3)_3C^+Cl^-$ in water.[5] With $(CH_3)_3C^+$ the preference for specific hydration on both sides of the carbenium carbon yields a sharper variation in the primary hydration numbers. The comparatively spherical tetramethylammonium ion lacks this orientational preference and the changes that occur between the contact and solvent-separated minima are less pronounced.

Chloride Ion Pairs. A. Potential of Mean Force. The potential of mean force for the chloride–chloride interaction in water is shown in Figure 10, anchored to the primitive model result at 8.2 Å. The incremental and total free energy changes obtained from the simulations along with the fluctuations ($\pm 1\sigma$) from averages over separate blocks of 2×10^5 configurations are listed in Table IV. The cumulative uncertainty in the potential of mean force is estimated to be ca. ±0.5 kcal/mol at the endpoints relative to the middle. The results indicate the presence of a free energy

Table IV. Results for the Potential of Mean Force for $Cl^-\cdots Cl^-$ in a Box of 250 (top) and 750 (bottom) Water Molecules from the Monte Carlo Simulations[a]

r(Cl–Cl)		ΔG		
r_i	r_j	$i \rightarrow j$	$j \rightarrow i$	ΔG^{tot}
3.4	3.6		6.96 ± 0.15	12.14
3.6	3.8	−3.82 ± 0.17		5.18
3.8	4.0		2.58 ± 0.21	1.36
4.0	4.2	−1.43 ± 0.17		−1.23
4.2	4.4		1.17 ± 0.20	−2.66
4.4	4.6	−0.45 ± 0.21		−3.83
4.6	4.8		0.44 ± 0.11	−4.28
4.8	5.0	0.33 ± 0.15		−4.72
5.0	5.2		−0.71 ± 0.24	−4.39
5.2	5.4	1.21 ± 0.16		−3.68
5.4	5.6		−0.44 ± 0.12	−2.47
5.6	5.8	0.40 ± 0.17		−2.03
5.8	6.0		−0.73 ± 0.12	−1.63
6.0	6.2	1.09 ± 0.22		−0.90
6.2	6.4		−0.35 ± 0.33	0.19
6.4	6.6	−0.08 ± 0.22		0.54
6.6	6.8		0.25 ± 0.14	0.46
6.8	7.0	−0.21 ± 0.11		0.22
7.0	7.2		−0.48 ± 0.31	0.09
7.2	7.4	0.28 ± 0.12		0.49
7.4	7.6		−0.50 ± 0.30	0.77
7.6	7.8	0.36 ± 0.19		1.27
7.8	8.0		0.85 ± 0.16	1.63
8.0	8.2	−0.78 ± 0.19		0.78
4.6	4.8		0.78 ± 0.09	
4.8	5.0	−0.05 ± 0.11		
5.0	5.2		−0.10 ± 0.14	
5.2	5.4	0.42 ± 0.15		

[a] Energies in kcal/mol; distances in Å.

minimum at an interionic separation of 4.8 Å with a ca. 6 kcal/mol barrier to escape. The well depth of 4.2 kcal/mol in the figure may be exaggerated by the anchoring to the primitive model at 8.2 Å. If the Monte Carlo result continues to descend more rapidly and level off beyond that point, it would diminish the well depth. However, it seems unlikely that variations in solvation beyond 8.2 Å would be large enough to raise the minimum at 4.8 Å above the free energy zero. Thus, there appears to be a Cl_2^{2-} aggregate that is bound in water relative to infinite separation of the ions. Though precedented,[6-8] the result is still surprising and we did want to test if the existence of the minimum was an artifact of the system size or cutoffs of the potential functions. Thus, two additional simulations with 750 water molecules and 2 Å longer cutoffs (10.5 Å) were run in the vicinity of the putative minimum. The results of these calculations are also listed in Table IV and are in satisfactory agreement with the findings for the smaller system. A minimum is still apparent, though it is now near 5.0 Å. Consequently, if the minimum is a computational artifact, it most likely arises from the lack of explicit polarization in the calculations. When the like-charged ions are close, the nearby water molecules are strongly polarized. This enhances the ion–water interactions, but it also causes many water–water interactions to become less favorable. The viability of the minimum depends on the balance of these opposing effects.

It is believed that the stabilization of the chloride ion pair in aqueous solution is a result of highly favorable bridging configurations in which water molecules are simultaneously hydrogen bonded to both chloride ions.[8] The optimal Cl–O distance found from the present potential functions is 3.2 Å for the linear Cl^-–water hydrogen bond.[25b] A structure in which a water molecule uses both hydrogens to linearly hydrogen bond to two chloride ions would then require an interionic distance of 5.0–5.1 Å, i.e., close to the location of the minimum in the calculated pmf.

B. Energy Distributions. The solute–solvent energy distributions, shown in Figures 11 and 12, provide additional insight into the mechanism of hydration which stabilizes the dianion pair. The individual ion pair–water interaction energy distributions are plotted in Figure 11 for several interionic separations: 4.4 Å (near

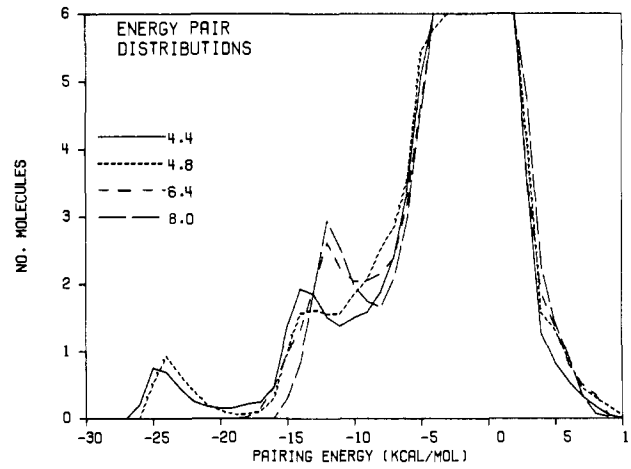

Figure 11. Distributions of individual water–ion pair interaction energies for $Cl^-\cdots Cl^-$ in water. The different curves are for the indicated Cl–Cl distances. Units as in Figure 6.

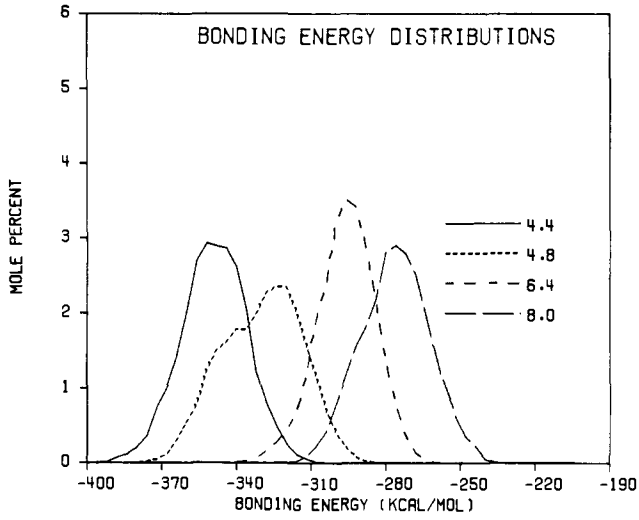

Figure 12. Distributions of total ion pair–solvent bonding energies for $Cl^-\cdots Cl^-$ in water.

the minimum), 4.8 Å (the free energy minimum), 6.4 Å (the barrier region), and 8.0 Å (the largest separation studied). The low-energy bands centered at ca. −24 kcal/mol for 4.4 and 4.8 Å correspond to bridging water molecules. The peak is nicely resolved for the minimum at 4.8 Å and its integral indicates that 3.0 water molecules participate in the bridging structures. The ion pair for r(Cl–Cl) equal to 4.4 Å still has ca. 2.7 bridging water molecules; however, the distributions at the separations beyond 4.8 Å resemble energy pair distributions for dilute chloride ion solutions.[24b] The band for the bridging water molecules is gone, while the band centered near −12 kcal/mol corresponds to water molecules bonding to a single chloride ion.[25b] The existence of the bridging water molecules for separations near the free energy minimum is clearly apparent in stereoplots of configurations from the simulations. Figure 13 shows a configuration for the chloride ion pair at the minimum. The three bridging water molecules are evident along with 3–4 additional water molecules hydrogen bonding to each ion. The novel structure can be called a "solvent-bridged" ion pair. A plot of a configuration at a chloride–chloride distance of 7.2 Å (Figure 14) shows that the bridging waters are absent and the two ions are independently solvated with the water molecules between the ions less than optimally oriented with respect to one another or the more distant ion.

The solute–solvent bonding energy distributions are displayed in Figure 12. In contrast to Figure 5, the average solute–solvent energy now becomes more favorable as the ions approach. This change of ca. 100 kcal/mol over the range is offset by increasing ion–ion repulsion and solvent disruption as the ions get closer.

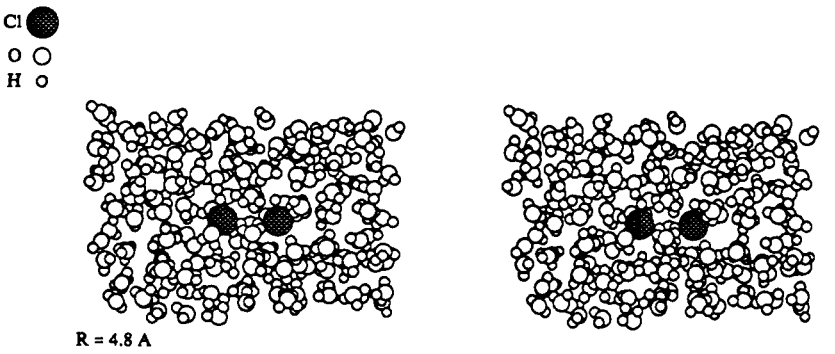

Figure 13. Stereoplot of a configuration for the $Cl^-\cdots Cl^-$ solvent-bridged ion pair at a separation of 4.8 Å. Water molecules more than 3.8 Å in front of either chlorine have been deleted for clarity.

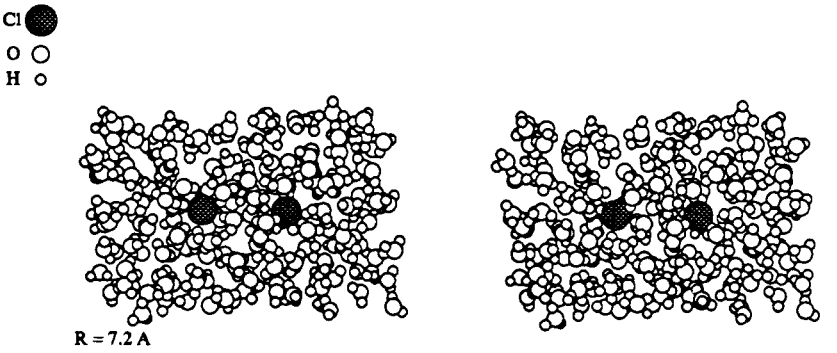

Figure 14. Stereoplot of the $Cl^-\cdots Cl^-$ ion pair at a separation of 7.2 Å. Details as in Figure 13.

Table V. Computed Coordination Numbers for $[Cl^-\cdots Cl^-]$ from Integrating the First Peaks in the Cl–O Radial Distribution Functions to 3.85 Å

r(Cl–Cl), Å	coord no Cl–O	r(Cl–Cl), Å	coord no Cl–O	r(Cl–Cl), Å	coord no Cl–O
3.6	7.4	5.2	7.5	6.8	7.7
4.0	8.0	5.6	7.8	7.2	7.1
4.4	8.1	6.0	7.2	7.6	7.0
4.8	7.2	6.4	7.8	8.0	8.3

C. **Atomic Distributions.** The Cl–O radial distribution functions at the same separations as above are displayed in Figure 15. The peaks in the Cl–O and Cl–H rdfs occur in the same locations as those for dilute aqueous Cl^-[25b] and reflect the prevalence of linear hydrogen bonding with water, The area under the first peak in the Cl–O rdf fluctuates between 7 and 8 water molecules (Table V). Thus, each chloride ion has its full complement of first-shell water neighbors at all interionic distances.

Proximity analyses performed on saved configurations further confirm the conclusions drawn about the structure and energetics of hydration. The computed primary and secondary coordination numbers are given in Table VI along with average interaction energies between the ion pair and water molecules in the primary shell. The number of molecules in the primary hydration shell reaches a minimum of ca, 5 in the solvent–bridged well, while the secondary hydration number simultaneously reaches a maximum of ca. 1.5. This means that each chloride ion has ca. 1.5 water oxygens within 3.85 Å that are closer to the other ion, as expected for the two ions sharing three bridging water molecules. As the ions separate and become independently solvated, the primary hydration number increases to 7–8 and the secondary hydration number goes to 0. The average ion pair–water interaction energies are also found to become less favorable as the ions separate and it becomes more difficult for the water molecules to orient favorably with respect to both ions and simultaneously fit into the water network.

D. Comparison to Earlier Studies. Our results are in qualitative agreement with the previous extended RISM calculation[6] and the molecular dynamics simulation.[7,8] These calculations both predicted the existence of a free energy minimum ca. 1 kcal/mol below the free energy of the fully separated ions. However, both found the minimum to occur at an interionic distance of ca. 3.6 Å, well inside the 4.8–5.0 Å reported here. The former separation is surprisingly small in view of the Lennard-Jones σ of 4.4 Å that

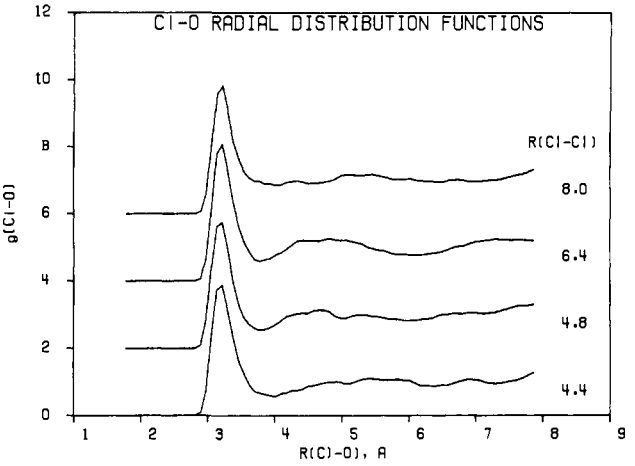

Figure 15. Cl (from $[Cl^-]_2$)–water O radial distribution functions computed in the simulations. Successive curves are offset 2 units on the y axis.

Table VI. Computed Hydration Numbers and Interaction Energies (kcal/mol) for $[Cl^-\cdots Cl^-]$ from Proximity Analyses

r(Cl–Cl)	primary hydration no.	secondary hydration no.	ion pair–water energy
3.6	6.3	1.3	−15.6
4.4	5.9	1.7	−15.4
4.8	5.2	1.5	−15.1
5.2	6.7	1.2	−14.0
5.6	6.5	0.5	−12.3
6.0	6.9	0.5	−12.1
6.4	6.8	0.5	−11.5
6.8	7.3	0.0	−10.7
7.2	8.0	0.0	−10.5
7.6	6.8	0.0	−10.8
8.0	7.4	0.0	−10.2

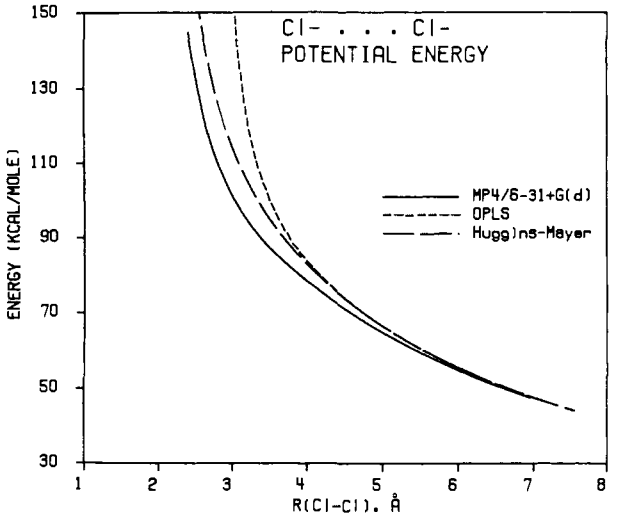

Figure 16. Potential energies for the chloride–chloride interactions predicted by the OPLS potential functions, the Huggins–Mayer model (ref 6), and MP4/6-31+G(d) ab initio calculations.

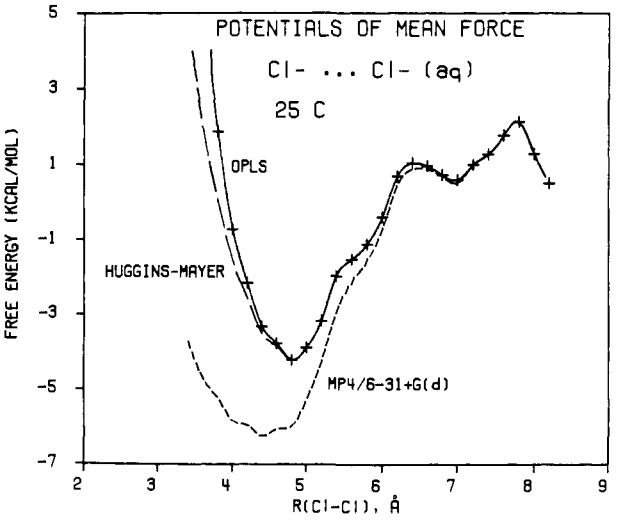

Figure 17. Calculated potentials of mean force using the Cl^-–Cl^- potentials in Figure 16 and the relative free energies of hydration computed in this work.

has been found appropriate for aqueous chloride ion.[25] Though we do not fully understand the origin of the discrepancy, some insights can be gained from a comparison of the potential functions. The water model in the Pettitt–Rossky study was a modification of the TIPS 3-site potential.[37] The solute–solvent potential parameters were fit to experimental data and results of ab initio calculations, while the $Cl^-\cdots Cl^-$ interactions were described by a Huggins–Mayer potential and based on crystal data for alkali chlorides. In Figure 16 the OPLS potential energy for $Cl^-\cdots Cl^-$ is compared to that from the Huggins–Mayer model and from the present quantum mechanical calculations (MP4/6-31+G(d)). The OPLS potential is more repulsive at short range than the Huggins–Mayer potential which is in turn more repulsive than the ab initio results. In order to determine the effect of the differing interionic interactions on the present results, the OPLS ion–ion potential was replaced by the others to yield the modified pmfs in Figure 17. Use of the quantum mechanical potential moves the minimum in by ca. 0.4 Å and deepens the well by 2 kcal/mol. However, replacement by the Huggins–Mayer potential has little effect on the entire pmf. In contrast, if the OPLS potential is used instead of the Huggins–Mayer alternative with the molecular dynamics results,[7] the free energy minimum in the MD results entirely disappears and the pmf is strictly repulsive.

(37) Jorgensen, W. L. *J. Am. Chem. Soc.* **1981**, *103*, 335.

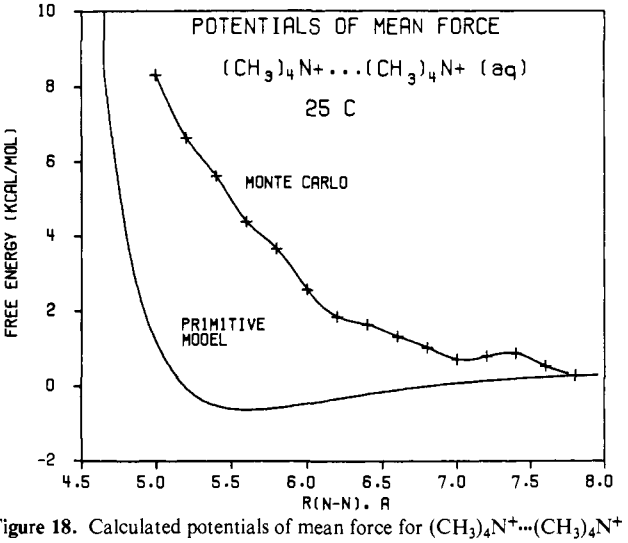

Figure 18. Calculated potentials of mean force for $(CH_3)_4N^+\cdots(CH_3)_4N^+$ in water.

Table VII. Optimized Geometries and Interaction Energies for $Cl^-\cdots H_2O$

potential model	r(Cl–H)	∠Cl–H–O	ΔE (kcal/mol)
OPLS	2.25	161	−13.17
Pettitt–Rossky	2.42	146	−14.49

Table VIII. Results for the Potential of Mean Force for $[(CH_3)_4N^+]_2$ from the Monte Carlo Simulations[a]

r(N–N)		ΔG		
r_i	r_j	$i \rightarrow j$	$j \rightarrow i$	$\Delta G^{tot}(r_i)$
5.0	5.2		1.67 ± 0.07	8.04
5.2	5.4	−1.03 ± 0.08		6.37
5.4	5.6		1.22 ± 0.15	5.34
5.6	5.8	−0.72 ± 0.12		4.12
5.8	6.0		1.10 ± 0.08	3.40
6.0	6.2	−0.72 ± 0.06		2.30
6.2	6.4		0.21 ± 0.15	1.58
6.4	6.6	−0.32 ± 0.13		1.37
6.6	6.8		0.29 ± 0.12	1.04
6.8	7.0	−0.33 ± 0.14		0.75
7.0	7.2		−0.09 ± 0.09	0.42
7.2	7.4	0.08 ± 0.08		0.50
7.4	7.6		0.33 ± 0.09	0.58
7.6	7.8	−0.25 ± 0.06		0.25

[a] Energies in kcal/mol; distances in Å.

This is a consequence of the much steeper slope with the OPLS potential near 3.5 Å as shown in Figure 16. Thus, the position and even occurrence of minima in the pmfs is sensitive to details of the gradients of the component interactions. Under the circumstances, it is well-advised to be consistent in the choice of functional form for the potential functions, as has been done here by using the Coulomb plus 12-6 Lennard-Jones format for all interactions (eq 1). On the other hand, mixing, for example, exp −6 and 12–6 terms for short-range interactions might lead to some imbalances and extraneous features in pmfs. In the extended RISM and MD studies, the ion–water and water–water interactions use the 12–6 form, while the ion–ion interaction has the softer exp–6 form.[6-8]

Hydration of the ions is also described differently by the two models. A comparison of the optimal geometry and interaction energy for a single chloride ion and one water molecule as determined by the OPLS potentials and by the Pettitt–Rossky model is given in Table VII. The pettitt–Rossky model favors longer, less linear hydrogen bonds. The combined effect of more bent hydrogen bonds in the bridging structure and the softer ion–ion potential for the Pettitt–Rossky model may account for the occurrence of the free energy minimum at smaller Cl–Cl distance in the previous studies.

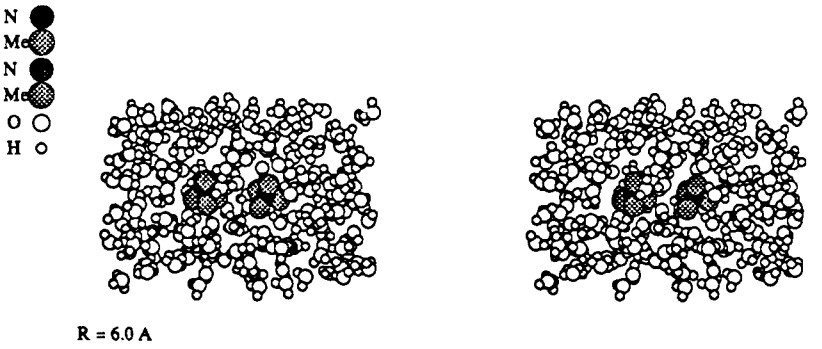

Figure 19. Stereoplot of a configuration for $(CH_3)_4N^+\cdots(CH_3)_4N^+$ at an N–N separation of 6.0 Å. Water molecules more than 4.5 Å in front of either nitrogen have been deleted for clarity.

Tetramethylammonium Cation Pairs. A. Potential of Mean Force. The computed potential of mean force for $(CH_3)_4N^+\cdots(CH_3)_4N^+$ is shown in Figure 18, anchored to the primitive model result at 7.8 Å. The numerical details are tabulated in Table VIII. The cumulative fluctuation at the endpoints relative to the middle is ±0.2 kcal/mol. The free energy curve is found to be repulsive and pushed out significantly from the primitive model result. This is again attributable to the shielding effect the ions have on one another. No contact minimum is detected; solvent bridging would not be viable for this system. The RHNC study detected a shallow minimum for the model $(C_2H_5)_4N^+$ ion pairs that was negligibly stabilized with respect to infinite separation and pushed out from contact by ca. 0.2 solvent diameters.[9]

B. Bonding Energy Distributions. The solute–solvent bonding energy distributions are comparatively featureless and are not illustrated here. The total ion pair–water interaction energy declines from about −160 kcal/mol at r(N–N) = 7.6 Å to about −195 kcal/mo at 5.2 Å. So, the variation is not as great as for the Cl^- pair (Figure 12) since the individual ion–water interactions are weaker for the tetramethylammonium ion. Furthermore, the distribution of individual ion pair–water interaction energies is now essentially featureless in comparison to Figure 11. There is just one band spanning from ca. −14 to +7 kcal/mol at all interionic distances. The band does extend more to low energy for shorter interionic spearations, which indicates that there are more interactions where water molecules interact favorably with both ions when the ions are close. Nevertheless, this effect is not enough to offset the concomitant increases in the ion–ion repulsion and destabilization of the water network.

C. Structural Analysis. The N–O, N–H, CH_3–O, and CH_3–H rdfs are similar to those for a dilute aqueous solution of $(CH_3)_4N^+$ and change little with ion separation.[25a] Integration yields a methyl group coordination number that fluctuates around 7–8, while proximity analysis gives a primary hydration number of ca. 4 with a cutoff of 4.5 Å. The average interaction energy between the ion pair and water molecules in the primary shell increases as a function of ion separation from −4.1 kcal/mol for r(N–N) = 5.2 Å to −3.1 kcal/mol at 7.6 Å. This pattern was also observed for the chloride ion dimer (Table VI) and arises from the increasing difficulty of orienting water molecules to interact favorably with both ions as the interionic distance increases or, in other words, from the unfavorable overlap of solvent cages as the ions become independently solvated. A configuration at 6.0 Å is shown in Figure 19. At this point, the ions are beginning to form separate hydration shells and the water molecules between the ions appear to clearly favor interactions with one ion while nicely maintaining the hydrogen-bonded network of water.

It is interesting to note that previous theories of hydration based on Gurney cosphere overlap predict less favorable hydration layer overlap for two chloride ions than for tetramethylammonium ions.[35] The earlier theory does not consider the existence of the bridging structures and overestimates the hydrophobic effect for the tetramethylammonium cations.

Concluding Remarks

Including the results reported here, Monte Carlo and molecular dynamics simulations have so far been used to compute only six interionic potentials of mean force.[4,5,7] Though such calculations are clearly at an incipient stage, the approach is promising and the initial results have been provocative. Some patterns have also begun to emerge. For oppositely charged ions in water, the occurrence of free energy minima for both contact and solvent-separated ion pairs is the general rule. In each of the three cases that have been studied, the barrier between the contact and solvent-separated forms has been no more than 3 kcal/mol. For like-charged ions, the results are surprisingly variable for the two available cases. Consistent with experimental findings,[16-21] the present results indicate that the smallest of the tetraalkylammonium ions has no tendency toward self-association in water. However, in support of the earlier molecular dynamics results,[7] a stable solvent-bridged ion pair is predicted for two chloride ions in water. Though some experimental evidence has been presented for halide ion associations,[22] more direct support or refutation[23] of the theoretical predictions is needed. The theoretical results again raise the possibility of other stable like-charged ion pairs. Though integral equation results indicate that this is unlikely for alkali ions in water,[6,9] there is evidence for the association of large, "hydrophobic" ions[9,17-22] and some metal ions.[38]

The simulation work has also helped elucidate the changes in hydration as a function of interionic distance. The hydration of the oppositely charged pairs becomes less favorable as the ions approach since the solvent dipoles for the two hydration spheres are oriented unfavorably for interaction with the other ion except for the few solvent molecules that may be directly between the ions. On the other hand, the hydration of the like-charged ion pairs becomes more favorable as the ions approach. When the ions are near contact, the solvent dipoles can be readily aligned to interact well with both ions. However, as the ions separate, solvent molecules between the ions cannot orient their dipoles to interact favorably with both ions. This effect coupled with water bridging could lead to a significant barrier to negative ion pair dissociation in aqueous solution. A key question is the relative free energy for the resultant minimum versus the fully separated ions.

Finally, although the initial results have been intriguing, the limitations of the calculations are significant. The finite system sizes, cutoffs, and lack of explicit polarization are the major concerns, though some cancellation of the associated errors can be expected owing to ther nature of perturbation calculations. Nevertheless, until these issues can be better treated, it is advisable to apply the calculations to relatively large, charge-delocalized ions.

Acknowledgment. Gratitude is expressed to the National Science Foundation and the National Institutes of Health for support of this research. Fellowship support was kindly provided by Procter & Gamble, Inc. Enlightening comments from Professors H. L. Friedman and P. J. Rossky were also much appreciated.

Registry No. $(CH_3)_4N^+Cl^-$, 75-57-0.

(38) Friedman, H. L. *Faraday Discuss. Chem. Soc.* **1988**, *85*, 1. Neilson, G. W.; Enderby, J. E. *Proc. R. Soc. London, Ser. A* **1983**, *390*, 353.